Theoretical formulation of the distribution function of critical nuclei under precipitation polymerization conditions

Antonio L. Medina-Castillo [a],[*], Modesto T. Lopez-Lopez [b], María Dolores Fernandez-Ramos [a]

[a] *Universidad de Granada, Departamento de Química Analítica, Campus de Fuentenueva, E-18071, Granada, Spain*
[b] *Universidad de Granada, Departamento de Física Aplicada, Campus de Fuentenueva, E-18071, Granada, Spain*

ARTICLE INFO

ABSTRACT

Precipitation Polymerization (*Pre-Poly*) can be considered a nucleation and growth process in which complex and high molecular weight branched polymers are involved. From an experimental point of view, it is well-known that under *Pre-Poly* conditions the phase transition (nucleation) occurs in the first minutes of polymerization, and then a long growth stage is observed in which the critical nuclei simultaneously grow until reaching a highly monodisperse distribution of microspheres (characteristic mechanism of binodal decomposition). The high rate at which nucleation and growth processes usually take place when radical polymerization (extremely high polymerization rate) under *Pre-Poly* conditions is used, makes it very difficult to study experimentally some aspects of these processes, such as the size and concentration of critical nuclei, among others. Based on the thermodynamic principles of *Pre-Poly,* this analytical paper covers for the first time, to the best of our knowledge, the theoretical formulation of the distribution function of critical nuclei under *Pre-Poly* conditions. In addition, a simple empirical method to calculate the concentration of critical nuclei was also developed using only three global, physical experimental parameters, and good agreement was found between empirical and theoretical calculations.

1. Introduction

Nucleation is a very common process in nature that has many practical consequences in science and technology [1,2]. In materials science, the casting of metals gives physical properties that depend on the conditions of crystal growth. In atmospheric sciences, the nucleation of both water droplets and ice crystals in the atmosphere has an important effect both in the short-term on the weather and in the long-term through global warming (or cooling) by cloud formation caused by atmospheric aerosols. In biology, there is much interest in bypassing nucleation of ice in the cryopreservation of human hues, and protein crystallization [1,2]. In polymer science, Precipitation Polymerization (*Pre-Poly*) is a nucleation and growth process in which complex high molecular weight branched polymers are involved, and it is unique to prepare polymeric microspheres with controlled and uniform size in the absence of any surfactant or additive for a wide range of applications [3–10].

According to the IUPAC *Pre-Poly* is a polymerization process in which monomers and initiator are dissolved in a given solvent (in the absence of any stabilizer or additive), and this continuous phase is a non-solvent for the formed polymer chains beyond a critical molecular weight [11]. Elucidate and understanding the nucleation and growth mechanisms under *Pre-Poly* conditions is an important issue both from a basic science point of view and to advance its experimental applications. In a previous work, the thermodynamic principles of *Pre-Poly* were successfully described by combining Scaling theory and Gibbs-Thompson formalism [12]. To this purpose, *Pre-Poly* was undertaken in three steps. I) Coil-to-Globule transition: partial desolvation/collapse of polymer chains occurs to form a monophasic dilute solution of globules. II) Phase transition (nucleation): self-assembly of the globules is produced, resulting in a suspension (biphasic system) of critical nuclei. III) Growth: new globules are formed which adhere to the surface of the critical nuclei.

In the thermodynamic description of polymer solutions, the classical Flory-Huggins theory (FHT) is only valid for usual linear chains, and for branched chains for high space dimensions ($d > 6$) [13]. For the usual dimension ($d = 3$) branched polymers, the classical theory does not work [13–15]. Scaling theory [16,17] is the simplest theoretically and is successfully used to describe the critical phenomena of coil-to-globule transition at the usual dimension ($d = 3$) of branched polymers

---

(purely branched; *RBP* and partially branched; *RBP_{b-t}*) [15,18,19]. Once the coil-to-globule transition occurs, phase transition (nucleation) is driven by the lowering of the free energy as the new phase forms; close to the equilibrium transition point, the original single-phase remains metastable, however, a fluctuation is required to cause the appearance of the first region of the new phase [20,21]. Under *Pre-Poly* conditions, nucleation strongly depends on interfacial effects occurring between globules and solvent molecules, named Gibbs–Thomson effects [20]. Therefore, Scaling theory and Gibbs-Thompson formalism have proved to be the appropriate theoretical framework to describe the critical phenomena of coil-to-globule transition and phase transition (nucleation) under *Pre-Poly* conditions [12].

Experimentally it is well-known that under *Pre-Poly* conditions the phase transition (nucleation) occurs in the first minutes of polymerization, and then a long growth stage is observed in which the critical nuclei simultaneously grow until reaching a highly monodisperse distribution of microspheres (characteristic mechanism of binodal decomposition) [12,22,23]. The high rate at which nucleation and growth processes usually take place when radical polymerization under *Pre-Poly* conditions is used, makes it very difficult to study some aspects of these processes, such as the size and concentration of critical nuclei, among others. For this reason, this paper covers the theoretical formulation of the distribution function of critical nuclei under *Pre-Poly* conditions, from a thermodynamics point of view. In addition, a simple empirical method to calculate the concentration of critical nuclei for a given *RBP_{b-t}* under *Pre-Poly* conditions using only three global, physical experimental parameters was also developed, and good agreement was found between empirical and theoretical calculations.

2. General thermodynamic aspects of precipitation polymerization

Before going into the theoretical formulation of the distribution function of critical nuclei under *Pre-Poly* conditions, we will introduce some of the general thermodynamic aspects of *Pre-Poly* [12]. Throughout this work, the sign $\approx$ is used to indicate that two quantities are proportional to each other by a dimensionless constant, and the sign $\cong$ indicates a numerical approximation. It should be noted that the theoretical aspects of this work are only valid in the case of polymeric

chains growing in poor solvents ($0.5 < \chi < \chi_{non-solvent}$). When the system crosses over from poor solvent to non-solvent ($\chi \geq \chi_{non-solvent}$) the attraction dominates completely, the individual chains have a fully collapsed conformation, and aggregation phenomena occur in an uncontrolled manner [12]. The presence of a multi-functional monomer (cross-linker) is commonly used in precipitation polymerization [5,7], thus, in this work the growing polymeric chains are considered as randomly partially branched chains (RBP_{b-t}) which can be represented by an equivalent chain formed by N unit of b length (Kuhn Length) [12]. Fig. 1 shows a scheme of *Pre-poly* process.

The crossover of polymer chains from dilute-θ regimen to the collapsed state depends on the length of the chain [18,19]. Thus, under *Pre-Poly* conditions the polymer chains are growing solvated until reaching the critical molecular weight ($N_{\theta,F}$: number of Kuhn segments of the critical chain; just before the collapse is produced), which may be written as [12]

$$N_{\theta,F} = C_1 \frac{1}{(2\chi - 1)^{16/11} \Lambda^{3/11}} \tag{1}$$

Where, χ, Λ, and C_1 are Flory Interaction Parameter, the fraction of branching points in the chain (Λ depends on the initial concentration of crosslinker) [12] and a dimensionless proportionality constant, respectively. After reaching $N_{\theta,F}$, the collapse of the polymer chain (globule formation) is produced by a small increase in $N_{\theta,F}$ ($N_{\theta,F} + \Delta N$; $\Delta N \ll N_{\theta,F}$): see step (2) of Fig. 1, and the size of the globule may be expressed as [12]

$$R_G(\chi) \approx \frac{b}{(2\chi - 1)^{9/11} \Lambda^{1/11}} \tag{2}$$

Where b is Kuhn length. As shown in Fig. 2, under *Pre-Poly* conditions, coil-to-globule transition can be considered a cyclic process [12]. The surface energy per unit of area (γ) of a globule is of the order of kT per thermal blob at the surface [24,25]

$$\gamma \approx \frac{kT}{b^2}(2\chi - 1)^2 \tag{3}$$

and the total surface energy of a globule, E_γ, is the product between γ and the globule surface area: R_G^2. Thus, by eqs 2 and 3, E_γ may be written as
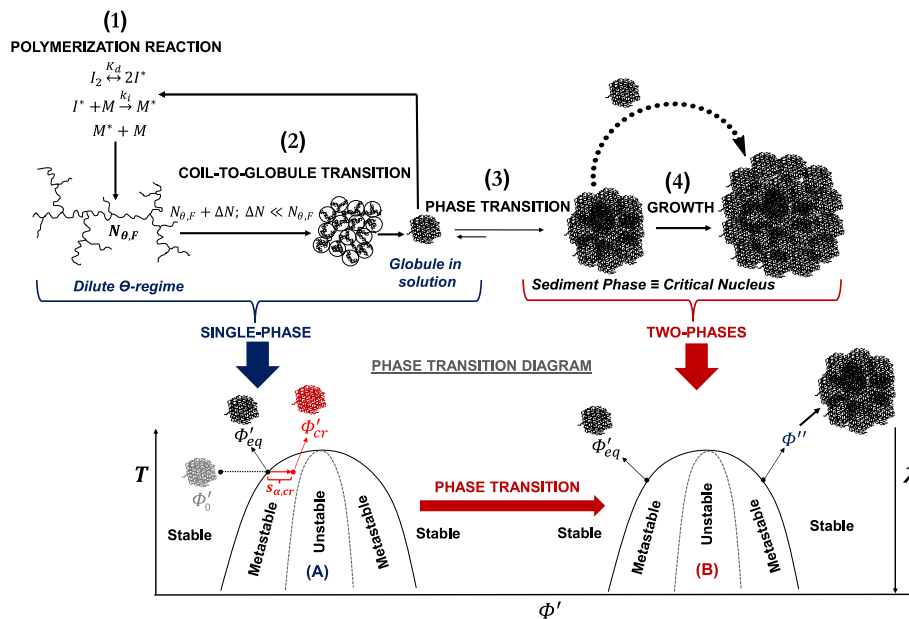
Fig. 1. Cyclic process of coil-to-globule transition ($N_{\theta,F}$ is the critical molecular weight) (**1**) and (**2**), Phase transition (nucleation) (**3**), Growth of critical nuclei (**4**). Phase Transition Diagram (**A**) $s_{\alpha,cr}$ is the critical fluctuation, which represents the amplitude of the fluctuation of the concentration of globules in the metastable region, Phase Transition Diagram (**B**) represents the nucleation process; Φ^* is the volume fraction of polymer of critical nuclei.
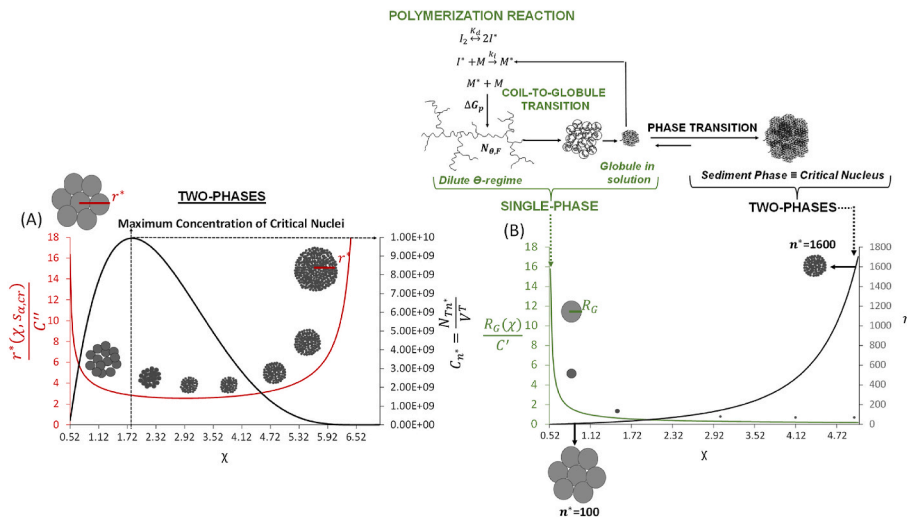
Fig. 2. Theoretical simulation of the distribution function of critical nuclei $\left(C_{n^*} = \frac{N_{Tn^*}}{V_T}\right)$ (see eq (22)), the radius of critical nuclei $\left(\frac{r^*(\chi, s_{\alpha,cr})}{C'}\right)$ (see eq (10)) (A), the radius of the globule $\left(\frac{R_G}{C'}\right)$ (see eq (2)), and the number of globules per critical nuclei (n^*) (see eq (12)) (B). For the simulations, the theoretical values of critical fluctuation $s_{\alpha,cr}$ versus χ were obtained by eq (5), and the value of constant K_1 of eq (22) ($K_1 = 5 \times 10^{13}$ *critical nuclei* cm^{-3}) was calculated by using the following values for the constant parameters: $C_2 \cong 4 \times 10^{-5}$, $C_1 \cong 1 \times 10^2$, $\rho_{poly} = 1.2$ gr cm^{-3}, $M_{w(mon)} = 1000$ gr mol^{-1}, and $\rho_{pK} = 0.74$, and $\Lambda = 0.35$.

$$E_\gamma = \gamma R_G^2 \approx kT \frac{(2\chi - 1)^{4/11}}{\Lambda^{2/11}} \tag{4}$$

Owing to the high cost of their surface energy, the equilibrium concentration of the globules in solution is very low (globules would like to stick together forming large cluster with lower value of E_γ, and their high surface energy can only be balanced by their translational entropy [24]. Therefore, at the beginning of the polymerization, the concentration of globules (Φ'_0) is very low, and thus their translational entropy is very high, so they remain solvated (single-phase solution: see Fig. 1; Phase Transition Diagram **A**). When the globules reach the equilibrium concentration (Φ'_{eq}), there is a thermodynamically metastable fluctuation of the concentration of globules (critical fluctuation; $s_{\alpha,cr}$) until the critical concentration (Φ'_{cr}) is reached (see Fig. 1; Phase Transition Diagram **A**). The critical fluctuation, $s_{\alpha,cr}$ represents the amplitude of the fluctuation of the concentration of globules in the metastable region (see Fig. 1; Phase Transition Diagram **A**), and it is a measure of the translational entropy of globule s whose value changes in the interval $0 < s_{\alpha,cr} < 1$. For a given RBP_{b-t} under *Pre-Poly* conditions, critical fluctuation can be expressed as a function of χ [12] by

$$s_{\alpha,cr} = 0.32 \frac{\Lambda^{2/11} \ln(-0.33\chi + 3.17)}{(2\chi - 1)^{4/11}}; \chi > 0.5 \tag{5}$$

once Φ'_{cr} is reached, phase transition (nucleation) occurs. During phase transition (nucleation) self-assembly of globules occurs to form the critical nuclei (sediment phase), and the concentration of globules returns to the equilibrium position; Φ'_{eq} (see Fig. 1: Phase Transition Diagram **B**). The released energy per globule ($\Delta G_{f,cr}$) due to the phase transition can be written as [12]

$$\Delta G_{f,cr} = -E_\gamma s_{\alpha,cr} \tag{6}$$

substituting E_γ by eq (4) into eq (6), $\Delta G_{f,cr}$ can be expressed as a function of interaction parameter; χ and critical fluctuation;

$$\Delta G_{f,cr}(s_{\alpha,cr}, \chi) \approx -\frac{kT s_{\alpha,cr}(2\chi - 1)^{4/11}}{\Lambda^{2/11}}; 0 < s_{\alpha,cr} < 1 \tag{7}$$

Then, volumetric energy: ΔG_v results from dividing eq (7) by the volume of the globule ($v'' = \frac{4}{3}\pi R_G^3$) [12]:

$$\Delta G_v(s_{\alpha,cr}, \chi) \approx -\frac{kT s_{\alpha,cr} \Lambda^{1/11} (2\chi - 1)^{31/11}}{b^3}; 0 < s_{\alpha,cr} < 1 \tag{8}$$

On the other hand, critical radius, r^*, is given by [26,27]

$$r^* = -\frac{2\gamma}{\Delta G_v} \tag{9}$$

substituting γ and ΔG_v by eqs 3 and 8 into eq (9), the radius of critical nucleus r^* may be written as

$$r^*(s_{\alpha,cr}, \chi) = \frac{8R_G}{3s_{\alpha,cr}} \approx \frac{b}{s_{\alpha,cr} \Lambda^{1/11} (2\chi - 1)^{9/11}}; 0 < s_{\alpha,cr} < 1 \tag{10}$$

Finally, the number of globules per critical nucleus (n^*) may be expressed as [12]

$$n^* = \rho_{pk}\left(\frac{r^*}{R_G}\right)^3 \tag{11}$$

Where ρ_{pk} is a dimensionless parameter that indicates the packing density of critical nuclei [26,27]. Substituting r^* and R_G by eqs 10 and 2 into eq (11), n^* can be expressed a

$$n^* = \frac{8}{27} \frac{\rho_{pk}}{s_{\alpha,cr}^3}; 0 < s_{\alpha,cr} < 1 \tag{12}$$

Since for a given RBP_{b-t} under *Pre-Poly* conditions the values of critical fluctuation, $s_{\alpha,cr}$ can be related to χ by eq (5), eq (7), 8, 10, and 12 can be transformed into a single variable (χ) equations, allowing to simulate the critical phenomena of coil-to globule transition and nucleation versus χ, as we will see in the next section.

3. Theoretical formulation of the distribution function of critical nuclei

The reasoning and deductions made in this section have been carried out assuming precipitation polymerization systems in which a distribution of highly monodisperse microspheres is formed. Based on the thermodynamic principles of *Pre-Poly* described in section 1, this section focuses on the theoretical formulation of the distribution function of critical nuclei under *Pre-Poly* conditions versus interaction parameter, χ and critical fluctuation, $s_{\alpha,cr}$. For this purpose, we will begin expressing the mass of a globule as follows:

$$m_G = m_{mon} N_G \tag{13}$$

Where m_{mon} is the mass of a single Kuhn segment and N_G is the total number of Kunt segment of the globule. Since the total collapse (branched and linear parts) of the polymer chains occurs spontaneously due to a very small fluctuation of the critical molecular weight ($N_{\theta,F} + \Delta N$; $\Delta N \ll N_{\theta,F}$) [12] (see Fig. 1), $N_{\theta,F}$ can be considered practically equal

to N_G:

$$N_G \cong N_{\theta,F} \tag{14}$$

Substituting now N_G by eq (1) into eq (13), we get

$$m_G = C_1 m_{mon} \left[\frac{1}{(2\chi - 1)^{16/11} \Lambda^{3/11}} \right] \tag{15}$$

On the other hand, the mass of a critical nuclei (m_{r^*}) can be expressed as

$$m_{r^*} = n^* m_G \tag{16}$$

Where n^* is the number of globules per critical nuclei (see eq (12)). Therefore, substituting n^* by eq (12) and m_G by eq (15) into eq (16), m_{r^*} may be written as

$$m_{r^*} = \frac{8 C_1 \rho_{pK} m_{mon}}{27 s_{\alpha,cr}^3} \left[\frac{1}{(2\chi - 1)^{16/11} \Lambda^{3/11}} \right] \tag{17}$$

The total number of critical nuclei (N_{Tn^*}) may be expressed as the ratio between the total mass of critical nuclei (m_n), and the mass of a critical nuclei (m_{r^*}):

$$N_{Tn^*} = \frac{m_n}{m_{r^*}} \tag{18}$$

On the other hand, for a RBP_{b-t} under *Pre-Poly* conditions, the total mass of critical nuclei is given by [12].

$$m_n = C_2 \rho_{poly} V_T (2\chi - 1) \left\{ exp\left[\frac{E_\gamma - \Delta G_{f,cr}}{kT} \right] - 1 \right\} \tag{19}$$

Where V_T, ρ_{poly}, E_γ (see eq (4)), $\Delta G_{f,cr}$ (see eq (7)) and C_2 are the total volume of the system, the polymer density, the surface energy of a globule, the released energy per globule due to the phase change, and a dimensionless proportionality constant, respectively. Therefore, substituting eqs 17 and 19 into eq (18) leads

$$C_{n^*} = \frac{N_{Tn^*}}{V_T} = \frac{27 C_2 \rho_{poly}}{8 C_1 \rho_{pK} m_{mon}} (2\chi - 1)^{27/11} \Lambda^{3/11} s_{\alpha,cr}^3 \left\{ exp\left[\frac{E_\gamma - \Delta G_{f,cr}}{kT} \right] - 1 \right\} \tag{20}$$

In eq (20), the ratio $C_{n^*} = \frac{N_{Tn^*}}{V}$ expresses the critical nuclei concentration for a given RBP_{b-t} under *Pre-Poly* conditions. Therefore, substituting now E_γ and $\Delta G_{f,cr}$ by eqs 4 and 7 into eq (20), C_{n^*} can be expressed as function of both the interaction parameter, χ, and the critical fluctuation $s_{\alpha,cr}$.

$$C_{n^*}(s_{\alpha,cr}, \chi) = \frac{27 C_2 \rho_{poly}}{8 C_1 \rho_{pK} m_{mon}} (2\chi - 1)^{27/11} \Lambda^{3/11} s_{\alpha,cr}^3 \, exp\Bigg[$$
$$- \frac{(2\chi - 1)^{4/11}}{\Lambda^{2/11}} \Bigg] \left\{ exp\left[\frac{s_{\alpha,cr}(2\chi - 1)^{4/11}}{\Lambda^{2/11}} \right] - 1 \right\} \tag{21}$$

For a given RBP_t under *Pre-Poly* conditions, the density of the polymer (ρ_{poly}) and the packing factor (ρ_{pK}) [26,27] of critical nuclei may be considered constant parameters [12], and eq (20) can be written as

$$C_{n^*}(s_{\alpha,cr}, \chi) = K_1 (2\chi - 1)^{27/11} \Lambda^{3/11} s_{\alpha,cr}^3 \, exp\Bigg[$$
$$- \frac{(2\chi - 1)^{4/11}}{\Lambda^{2/11}} \Bigg] \left\{ exp\left[\frac{s_{\alpha,cr}(2\chi - 1)^{4/11}}{\Lambda^{2/11}} \right] - 1 \right\} \tag{22}$$

Where the constant K_1 is a proportionality constant with units of inverse of volume.

3.1. Estimation of the order of magnitude of constant K_1

Bearing in mind that the mass of a monomer (m_{mon}) can be expressed

as the ratio between the molecular weight of the monomer (M_w) and Avogadro's number (N_A), the constant K_1 of eq (22) may be expressed as

$$K_1 = \frac{27 C_2 \rho_{poly} N_A}{8 C_1 \rho_{pK} M_{w(mon)}} \tag{23}$$

To estimate the theoretical order of magnitude of the constant K_1, Poly methyl methacrylate (PMMA; ρ_{poly} is 1.2 gr cm^{-3}) is used as polymer model (PMMA is widely used in *Pre-Poly*). On the other hand, a theoretical molecular weight of 1000 gr mol^{-1}, and a hexagonal close-packed (HCP; $\rho_{pK} = 0.74$) were assumed for the mass of Kuhn length ($M_{w(mon)}$) and critical nucleus, respectively. We want to highlight that our assumptions to estimate the order of magnitude of the constant K_1 are intuitive (derived from our experimental experience in Pre-Poly) but necessary, because to our knowledge, until now the experimental calculation of the critical molecular weight under Pre-Poly conditions is unfeasible.

In *Pre-Poly* the nucleation process is experimentally observed in the first minutes of polymerization, and then the critical nuclei exponentially increase in size over a long growth stage [12]. Therefore, the ratio between the radius of the final particles and the radius of the critical nuclei ($\frac{r_f}{r^*}$) is very high, which leads to a very low value of the proportionality constant C_2 of eq (19) (e.g., for $\frac{r_f}{r^*} = 15$, $C_2 \cong 4 \times 10^{-5}$) [12]. Finally, to estimate the order of magnitude of the constant C_1 of eq (1), let us assume a theoretical value of 100 units of b length (Kuhn length) for the critical molecular weight ($N_{\theta,F}$) when $\chi = 1$, which leads to $C_1 = 1 \times 10^2$. Thus, by using $C_2 \cong 4 \times 10^{-5}$, $C_1 \cong 1 \times 10^2$, $\rho_{poly} = 1.2$ gr cm^{-3}, $M_{w(mon)} = 1000$ gr mol^{-1}, and $\rho_{pK} = 0.74$, a theoretical value of 5×10^{13} critical nuclei cm^{-3} was obtained for the constant K_1.

3.2. Theoretical simulation of the coil-to-globule transition and nucleation process for a RBP_{b-t} under Pre-Poly conditions

By using eq (2) (radius of globule; R_G), eq (10) (radius of critical nucleus; r^*), eq (12) (number of globules per critical nucleus; n^*), eq (22) (distribution function of critical nuclei; C_{n^*}), and eq (5) that relate the values of critical fluctuation, $s_{\alpha,cr}$ versus χ, Fig. 2 Shows a theoretical simulation of the critical phenomena of coil-to-globule transition and nucleation (self-assembly of globules to form critical nuclei) for a given RBP_{b-t} versus χ under *Pre-Poly* conditions.

The size of the critical nucleus, r^* (see Fig. 2A; curve of $\frac{r^*(\chi, s_{\alpha,cr})}{C}$ vs χ) depends on both the size of the globule, R_G (see Fig. 2B; curve of $\frac{R_G}{C}$ vs χ) and the number of globules, n^* (see Fig. 2B; curve of n^* vs χ). For low values of χ ($0.52 \leq \chi \leq 1.00$) (low values of the total surface energy of a globule, E_γ; see eq (4)) the values of n^* are yet very low and remain practically constant with increasing χ however, in this region, χ has a very strong influence on the size of the globule, R_G. Under such conditions, the influence of n^* on r^* is negligible and the size of the critical nucleus is defined by the size of the globule. For intermediate values of χ ($1.00 \leq \chi \leq 2.95$) (intermediate values of the total surface energy of a globule, E_γ) both R_G and n^* change smoothly with increasing χ; n^* increases and R_G decreases, and r^* smoothly decreases with increasing χ until a minimum is reached when $\chi = 2.95$ (see Fig. 2A; curve of $\frac{r^*(\chi, s_{\alpha,cr})}{C}$ vs χ). Finally, for highest values of χ ($2.95 \leq \chi \leq 5.05$) (highest values of total surface energy of a globule, E_γ), the solvent is already extremely poor (globules are already very small and compact), and R_G remains practically constant with increasing χ (see Fig. 2B; curve of $\frac{R_G}{C}$ vs χ). Hence, in order to reduce efficiently the polymer surface area exposed to the solvent during the nucleation, n^* begins to increase abruptly, and consequently in this region r^* is defined only by n^* (see Fig. 2). For extremely high values of χ (non-solvent for the polymeric chains; $\chi \geq \chi_{non-solvent}$) the attraction dominates completely [24], resulting in an unstable suspension of critical nuclei: after nucleation, the critical nuclei stick together to further reduce the surface area exposed to the solvent,

leading to the formation of large and non-spherical aggregates) [12]. A Gaussian distribution with a maximum value at $\chi \cong 1.8$ is observed for the concentration of critical nuclei (see Fig. 2A; curve of $C_{n^*} = \frac{N_{Tn^*}}{V_T}$ *vs* χ and eq (22)). As expected, when χ reaches very high values, the total surface energy of a globule is extremely high (see eq (4)), and thus C_{n^*} reaches very low values in order to reduce efficiently the polymer surface exposed to the solvent, resulting in few critical nuclei formed by the self-assembly of many small, compact globules.

4. Empirical approach of the distribution function of critical nuclei under *Pre-Poly* conditions

In a suspension of monodisperse microspheres, the representative mass of polymer contained in a single microsphere (m_p) can be expressed as

$$m_p = C_p V_p \tag{24}$$

Where C_p is the concentration of polymer of a microsphere (ratio between the mass of polymer contained in a microsphere and the total volume occupied by the microsphere), and V_p is the volume occupied by a microsphere. Multiplying both members of eq (24) by the total concentration of microspheres, $\mathbb{C}_{Tp}$ (number of microspheres per unit of volume: $\mathbb{C}_{Tp} = \frac{\mathbb{N}_{Tp}}{V_T}$), leads to

$$\frac{m_p \mathbb{N}_{Tp}}{V_T} = \frac{\mathbb{N}_{Tp}}{V_T} C_p V_p \tag{25}$$

Where $\mathbb{N}_{Tp}$ is the total number of microspheres and V_T is the total volume. In eq (25) $m_p \mathbb{N}_{Tp}$ is the total mass of polymer contained in the suspension (M_{Tp}), and thus the right-hand side of eq (25) is equal to the mass of polymer per unit of volume $\left(\frac{M_{Tp}}{V_T}\right)$:

$$\frac{M_{Tp}}{V_T} = \mathbb{C}_{Tp} C_p V_p \tag{26}$$

Therefore, clearing $\mathbb{C}_{Tp} \left(\frac{\mathbb{N}_{Tp}}{V_T}\right)$ from eq (26) leads to

$$\mathbb{C}_{Tp} = \frac{M_{Tp}}{V_T C_p V_p} \tag{27}$$

Bearing in mind that C_p can be expressed as; $C_p = \phi'' \rho_{poly}$ [24], where ϕ'' is the polymer volume fraction of a microsphere (volume fraction of polymeric chains contained in a microsphere inside the volume spanned by the microsphere), and ρ_{poly} is the polymer density, eq (27) can be expressed as

$$\mathbb{C}_{Tp} = \frac{M_{Tp}}{V_T V_p \phi'' \rho_{poly}} \tag{28}$$

On the other hand, ϕ'' may be written as [24]

$$\varphi'' = \left\{ \begin{array}{ll} C_4 (2\chi - 1) & \text{if } 0.5 < \chi < \chi_{Non-Solvent} \\ 1 & \text{if } \chi = \chi_{Non-Solvent} \end{array} \right\} \tag{29}$$

Where C_4 is a dimensionless proportionality constant. Therefore, substituting ϕ'' by eq (29) and V_p by $\frac{4}{3}\pi(r_f)^3$ (r_f is the radius of the final microspheres) into eq 28

$$\mathbb{C}_{Tp} = K'' \frac{M_{Tp}}{(2\chi - 1)(r_f)^3}; \; K'' = \frac{3}{V_T 4\pi C_4 \rho_{poly}} \tag{30}$$

where K'' is a proportionality constant with units of inverse of mass. It has been experimentally demonstrated that for a *RBP*$_b$-t under *Pre-Poly* conditions, nucleation occurs only once in the first minutes of polymerization, and then the critical nuclei grow simultaneously during a long growth stage [12]. Therefore, it can be reasonably assumed that the number of critical nuclei reaching the final size (final microspheres) is

very high, and proportional to the total number of critical nuclei. Thus, the concentration of final microspheres ($\mathbb{C}_{Tp}$; see eq (30)) may be expressed as

$$\mathbb{C}_{Tp} = \Psi C_{n^*} (\chi, s_{a,cr}) \tag{31}$$

where Ψ is a dimensionless proportionality constant that indicates the fraction of critical nuclei that reaches the final size. Now substituting $\mathbb{C}_{Tp}$ by eq (30) into eq (31), leads to

$$K'' \frac{M_{Tp}}{(2\chi - 1)(r_f)^3} = C_{n^*} (\chi, s_{a,cr}); \; K''' = \frac{K''}{\Psi} \tag{32}$$

where K''' $\left(\frac{K''}{\Psi}\right)$ is a proportionality constant with units of inverse of mass. By using only three global, physical experimental parameters (M_{Tp}, χ and r_f) eq (32) allows us to relate the empirical values of $\frac{M_{Tp}}{(2\chi-1)(r_f)^3}$ calculated from precipitation polymerization of an experimental polymeric model in different solvents, with the theoretical values of the distribution function of critical nuclei obtained by eq (22). The experimental polymeric model selected (S1) is based on the precipitation polymerization of the monomers hydroxyethyl methacrylate (HEMA), methacrylic acid (MAA), and the bifunctional monomer (cross-linker) ethylene glycol dimethacrylate (EDMA) in different solvents, at a constant initial molar feed composition (22%MAA, 42%HEMA, and 36% EDMA; RBP_{b-t} = MAA-co-HEMA-co-EDMA). The total polymerization volume (V_T) was 14 mL, toluene (TOL), acetonitrile (ACN), 2-propanol (2-PrOH) and their mixtures were used as solvents, and the polymerization reactions were carried out at 75 °C without stirring. The characteristic Flory interaction parameter (χ_{ex}), hydrodynamic radius of final microspheres (r_f), polydispersity index (PDI), and total mass of polymer at full conversion (M_{Tp}) for the polymeric system S1 in different solvents were obtained from a previous work [12] and used to calculate the values of $K'' \frac{M_{Tp}}{(2\chi-1)(r_f)^3}$ (see Table 1). We emphasize that the empirical values of χ and $K'' \frac{M_{Tp}}{(2\chi-1)(r_f)^3}$ of Table 1 are qualitative values, which will be closer to quantitative values as the experimental system S1 approaches an ideal precipitation polymerization system [12].

The empirical values of $K'' \frac{M_{Tp}}{(2\chi_{ex}-1)(r_f)^3}$ are plotted together with the theoretical values of $C_{n^*}(s_{a,cr}, \chi)$ in Fig. 3.

As can be seen from Fig. 3, in the interval ($2.89 \leq \chi_{ex} \leq 4.50$) the experimental values deviate from the theoretical values, which could be due to deviations from ideality [12] of the experimental polymeric system S1. Changes in the polymerization solvent could introduce deviations in the values of χ_{ex}, and K'' by both thermodynamic factors (when the solvent mixtures deviates from a thermodynamically ideal mixture [12]) and kinetic factors (decreasing/increasing of the lifetime of living radical polymeric chains due to termination reactions by chain-transfer to solvent, modifications of the reactivity ratios of radical species, decrease/increase of decomposition temperature of radical initiator, etc [28–30]). Anyway, despite possible deviations from ideality, quite remarkably, we find a good correlation between the empirical values of $K'' \frac{M_{Tp}}{(2\chi-1)(r_f)^3}$ and the theoretical values of $C_{n^*}(s_{a,cr}, \chi)$ predicted by eq (22) (see Fig. 3), confirming that eq (32) could be used to carry out an empirical prediction of the concentration of critical nuclei for a given RBP_{b-t} under *Pre-Poly* conditions.

As shown in Fig. 2B; see curve of R_G *vs.* χ, for $\chi = 1.70$ the globules are already completely collapsed, and its size, R_G remains practically constant *vs.* χ, so it is quite reasonable to assume $\chi = 1.70$ as the limit at which the overlap volume fraction of the globule (volume fraction of a single globule inside its pervaded volume) reaches its maximum value: $\phi'' \cong 1$. For $\chi > 1.70$ the transition from very poor solvent to non-solvent is progressively produced. Thus, taking the extreme values ($\chi \cong 1.70$, $\phi'' \cong 1$) as the limit of poor solvent, the constant C_4 of eq (29) was

Table 1
Experimental data obtained from precipitation polymerization of system S1 indifferent solvents.

Φ_{PrOH}	Φ_{TOL}	Φ_{ACN}	$\chi_{ex}*$	$r_f(nm)$	PDI	$M_{Tp}(gr)$	$K'' \dfrac{M_{Tp}}{(2\chi_{ex}-1)(r_f)^3}$ (cm^{-3})
0.00	0.19	0.81	1.49	737 ± 49	0.010 ± 0.020	0.166 ± 0.005	K'' (2.35E+8)
0.00	0.26	0.74	1.70	683 ± 40	0.100 ± 0.020	0.174 ± 0.004	K'' (2.52E+08)
0.00	0.34	0.66	1.97	618 ± 33	0.098 ± 0.010	0.180 ± 0.007	K'' (2.63E+08)
0.00	0.47	0.53	2.44	548 ± 35	0.089 ± 0.010	0.180 ± 0.007	K'' (2.58E+08)
0.00	0.58	0.42	2.89	505 ± 46	0.050 ± 0.020	0.175 ± 0.004	K'' (2.53E+08)
0.00	0.67	0.33	3.32	505 ± 36	0.065 ± 0.030	0.165 ± 0.008	K'' (2.34E+08)
0.00	0.76	0.24	3.73	492 ± 50	0.085 ± 0.020	0.179 ± 0.012	K'' (2.36E+08)
0.00	0.91	0.09	4.56	507 ± 29	0.085 ± 0.030	0.224 ± 0.009	K'' (2.02E+08)
0.18	0.05	0.77	0.70	1077 ± 51	0.091 ± 0.010	0.090 ± 0.004	K'' (1.78E+08)
0.17	0.05	0.79	0.73	1057 ± 36	0.094 ± 0.010	0.090 ± 0.004	K'' (1.65E+08)
0.15	0.05	0.80	0.76	1204 ± 84	0.098 ± 0.010	0.115 ± 0.004	K'' (1.38E+08)
0.12	0.05	0.83	0.84	981 ± 83	0.091 ± 0.020	0.124 ± 0.003	K'' (1.71E+08)
0.09	0.05	0.86	0.90	973 ± 62	0.095 ± 0.010	0.129 ± 0.004	K'' (1.70E+08)
0.08	0.02	0.90	0.89	1128 ± 45	0.100 ± 0.010	0.144 ± 0.005	K'' (1.30E+08)
0.04	0.05	0.91	1.02	932 ± 62	0.082 ± 0.010	0.161 ± 0.005	K'' (1.89E+08)
0.02	0.05	0.93	1.08	831 ± 63	0.030 ± 0.020	0.147 ± 0.011	K'' 2.24E+08)
0.00	1.00	0.00	5.12	896 ± 82	0.101 ± 0.050	0.243 ± 0.007	K'' (3.92E+07)

$\chi_{ex}*$: Experimental Interaction Parameter of the polymeric system S1 in different solvents.
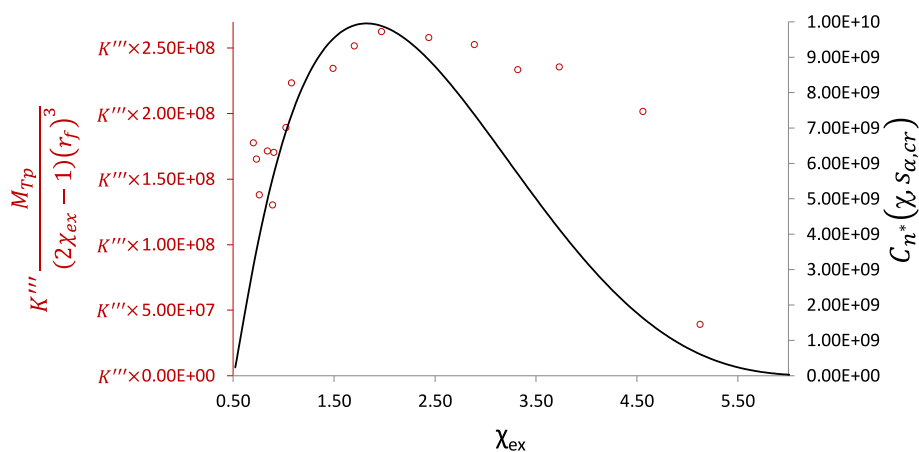
Fig. 3. Experimental values for the critical nuclei distribution function; $K'' \frac{M_{Tp}}{(2\chi_{ex}-1)(r_f)^3}$ (see **eq 33**), and theoretical values; $C_{n^*}(s_{\alpha,cr},\chi)$ (see eq (22)).

estimated; $C_4 = \frac{1}{(2 \times 1.70 - 1)} = 0.42$. Then, by using the total polymerization volume $V_T = 14$ mL, $C_4 = 0.42$, and $\rho_{poly} = 1.2$ gr cm^{-3} we obtained 33.8 gr^{-1} for K'' (see eq (30)). On the other hand, by extrapolating (in the interval $0.70 \le \chi_{ex} \le 1.70$) the theoretical values of C_{n^*} (see Fig. 2A; curve of C_{n^*} vs χ and eq (22)) and the corresponding experimental values of $\frac{M_{Tp}}{(2\chi_{ex}-1)(r_f)^3}$ (see Table 1) in eq (32), an average value of 34 gr^{-1} was obtained for the constant $K''' = \frac{K'}{\Psi}$, and thus 0.99 for $\Psi = \frac{K'}{K'}$, indicating that for the polymeric system S1, 99% of the critical nuclei formed during the phase transition (nucleation) simultaneously grow until reaching a similar final size, resulting in a monodisperse distributions of microspheres. This is in full agreement with the experimental results observed in precipitation polymerization [3–10,12], in which nucleation usually occurs in the first minutes of polymerization, and then a long growth stage is observed in which the critical nuclei simultaneously grow until reaching a highly monodisperse distribution of microspheres. Note that from a practical point of view, eq (32) may be useful to predict the radius of the final particle (r_f) at different experimental thermodynamic conditions.

5. Conclusions

Based on the thermodynamic principles of precipitation polymerization, for the first time, to the best of our knowledge, in this analytical paper the theoretical formulation of the distribution function of critical nuclei for a given RBP_{b-t} under *Pre-Poly* conditions has been carried out. In addition, a simple empirical method to predict the concentration of critical nuclei was also developed using only three global, physical experimental parameters: characteristic Flory interaction parameter (χ_{ex}), hydrodynamic radius of final microspheres (r_f), and total mass of polymer at full conversion (M_{Tp}). The analysis carried out shows a good correlation between the empirical and theoretical calculations, confirming that the empirical method reported could be used to carry out an experimental prediction of the concentration of critical nuclei for a given RBP_{b-t} under precipitation polymerization conditions.

CRediT authorship contribution statement

Antonio L. Medina-Castillo: Conceptualization, Writing – original draft, Software. **Modesto T. Lopez-Lopez:** Writing – review & editing, Data curation. **María Dolores Fernandez-Ramos:** Writing – review & editing, Data curation.

Declaration of competing interest

The authors declare that they have no known competing financial interests or personal relationships that could have appeared to influence the work reported in this paper.

Data availability

Data will be made available on request.

Acknowledgments

References

[1] J. Bai, Z. Shi, S. Jia, Y. Li, P. Peng, D. Xu, D.W. Oxtoby, Homogeneous nucleation: theory and experiment, J. Phys. Condens. Matter 4 (1992) 7627–7650, 10.1088/0953-8984/4/38/001.

[2] I.J. Ford, Nucleation theorems, the statistical mechanics of molecular clusters, and a revision of classical nucleation theory, Phys. Rev. E 56 (1997) 5615–5629, https://doi.org/10.1103/PhysRevE.56.5615.

[3] J. Wang, P.A.G. Cormack, D.C. Sherrington, E. Khoshdel, P.A.G. Cormack, J. Wang, D.C. Sherrington, E. Khoshdel, Monodisperse, Molecularly imprinted polymer microspheres prepared by precipitation polymerization for affinity separation applications, Angew. Chem. 115 (2003) 5494–5496, https://doi.org/10.1002/ange.200352298.

[4] A.H. Dam, D. Kim, Metal ion-imprinted polymer microspheres derived from copper methacrylate for selective separation of heavy metal ions, J. Appl. Polym. Sci. 108 (2007) 14–24, https://doi.org/10.1002/app.26923.

[5] W.-H. Li, H.D.H. Stöver, Monodisperse cross-linked core-shell polymer microspheres by precipitation polymerization, Macromolecules 33 (2000) 4354–4360, https://doi.org/10.1021/ma9920691.

[6] H. Kawaguchi, Functional polymer microspheres, Prog. Polym. Sci. 25 (2000) 1171–1210, https://doi.org/10.1016/S0079-6700(00)00024-1.

[7] E.C.C. Goh, H.D.H. Stöver, Cross-linked poly(methacrylic acid-co-poly(ethylene oxide) methyl ether methacrylate) microspheres and microgels prepared by precipitation polymerization: a morphology study, Macromolecules 35 (2002) 9983–9989, https://doi.org/10.1021/ma0211028.

[8] J.S. Downey, R.S. Frank, W.-H. Li, H.D.H. Sto, Growth mechanism of poly (divinylbenzene) microspheres in precipitation polymerization, Macromolecules 32 (1999) 2838–2844, https://doi.org/10.1021/ma9812027.

[9] A.L. Medina-Castillo, J.F. Fernandez-Sanchez, A. Segura-Carretero, A. Fernandez-Gutierrez, Micrometer and submicrometer particles prepared by precipitation polymerization: thermodynamic model and experimental evidence of the relation between flory's parameter and particle size, Macromolecules 43 (2010) 5804–5813, https://doi.org/10.1021/ma100841c.

[10] F. Bai, X. Yang, W. Huang, Synthesis of narrow or monodisperse poly (divinylbenzene) microspheres by distillation-precipitation polymerization, Macromolecules 37 (2004), https://doi.org/10.1021/ma048566l, 9746- 9742.

[11] S. Slomkowski, J. V Alemán, R.G. Gilbert, M. Hess, K. Horie, R.G. Jones, P. Kubisa, I. Meisel, W. Mormann, S. Penczek, R.F.T. Stepto, Terminology of polymers and polymerization processes in dispersed systems (IUPAC Recommendations 2011), Pure Appl. Chem. 83 (2011) 2229–2259, https://doi.org/10.1351/PAC-REC-10-06-03.

[12] A.L. Medina-Castillo, Thermodynamic principles of precipitation polymerization and role of fractal nanostructures in the particle size control, Macromolecules 53 (2020) 5687–5700, https://doi.org/10.1021/acs.macromol.0c00973.

[13] T.C. Lubensky, , et al.J. Vannimenus, Flory approximation for directed branched polymers and directed percolation, J. Phys., Lett. 43 (1982) 377–381, https://doi.org/10.1051/jphyslet:019820043011037700.

[14] T. Vilgis, P. Haronska, M. Benhamou, Branched polymers in restricted geometry : Flory theory, scaling and blobs, J. Phys. II 4 (1994) https://doi.org/10.1051/jp2:1994255ï.

[15] N.A. Makarevich, Nonideality factor in the thermodynamic analysis of real polymer solutions, Polym. Sci. 64 (2022) 128–144, https://doi.org/10.1134/S0965545X22020031.

[16] P.-G. de Gennes, Scaling Concepts in Polymer Physics, Cornell University Press, Ithaca, NY, 1979.

[17] P.-G. de Gennes, C.R. Hebd, Seances Acad. Sci., Ser. B (1980).

[18] M. Daoud, J. Joanny, J.F. Joanny, L. Léon Brillouin, C. Saclay, G. sur Yvette, Conformation of branched polymers, J. Phys. 42 (1981) https://doi.org/10.1051/jphys:0198100420100135900ï.

[19] M. Daoud, P. Pincus, W.H. Stockmayer, T. Witten, Phase separation in branched polymer solutions, Macromolecules 16 (1983) 1833. https://pubs.acs.org/sharingguidelines.

[20] M. Perez, Gibbs–Thomson effects in phase transformations, Scripta Mater. 52 (2005) 709–712, https://doi.org/10.1016/J.SCRIPTAMAT.2004.12.026.

[21] J.M. Stubbs, Y.G. Durant, D.C. Sundberg, Account/Revue Polymer phase separation in composite latex particles. 1. Considerations for the nucleation and growth mechanism, C. R. Chimie. 6 (2003), https://doi.org/10.1016/j.crci.2003.08.016.

[22] E.P. Favvas, A. Ch Mitropoulos, What is spinodal decomposition? J. Eng. Sci. Tech. Rev. 1 (2008) 25–27, https://doi.org/10.25103/jestr.011.05.

[23] T. Yao, A. Sen, A. Wagner, F. Teng, M. Bachhav, A. Ei-Azab, D. Murray, J. Gan, D. H. Hurley, J.P. Wharry, M.T. Benson, L. He, Understanding spinodal and binodal phase transformations in U-50Zr, Materialia (Oxf) 16 (2021), 101092, https://doi.org/10.1016/J.MTLA.2021.101092.

[24] M, C.R.H. Rubinstein, Polymer Physics, Oxford University Press, 2003.

[25] M. Kurata, Thermodynamics of Polymer Solution, CRC Press, New York, 1982.

[26] X. Bouju, É. Duguet, F. Gauffre, C.R. Henry, M.L. Kahn, P. Mélinon, S. Ravaine, Nonisotropic self-assembly of nanoparticles: from compact packing to functional aggregates, Adv. Mater. 30 (2018), https://doi.org/10.1002/ADMA.201706558.

[27] N.T.K. Thanh, N. Maclean, S. Mahiddine, Mechanisms of nucleation and growth of nanoparticles in solution, Chem. Rev. 114 (2014) 7610–7630, https://doi.org/10.1021/cr400544s.

[28] Y. Nakamura, S. Yamago, Termination mechanism in the radical polymerization of methyl methacrylate and styrene determined by the reaction of structurally well-defined polymer end radicals, Macromolecules 48 (2015) 6450–6456, https://doi.org/10.1021/acs.macromol.5b01532.

[29] W.K. Czerwinski, Solvent effects on free-radical polymerization. 6.f solvatochromic (LSER) analysis of the solvent effect on the homopolymerization rate on the basis of the reaction-solvent complex model, Macromolecules 28 (1995) 5405–5410. https://pubs.acs.org/sharingguidelines.

[30] A. Valdebenito, M.V. Encinas, Effect of solvent on the free radical polymerization of N,N-dimethylacrylamide, Polym. Int. 59 (2010) 1246–1251, https://doi.org/10.1002/PI.2856.